Stagnation-Point Heat-Transfer Measurements in Partially Ionized Air

P. H. Rose* and J. O. Stankevics†
Avco-Everett Research Laboratory, Everett, Mass.

Experimental measurements of convective stagnation-point heat transfer in partially ionized air at simulated flight velocities up to 55,000 fps are presented. Stagnation-point heat-transfer rates were measured in an arc-driven shock tube. The operation of this tube was carefully monitored by a variety of diagnostic techniques, and it is shown that auxiliary measurements must be made to identify those regions where ideal flow conditions exist. Calorimetric gages were used to measure heat-transfer rates. The effects of boundary-layer chemistry, radiation from the hot inviscid flow, and instrumentation errors are discussed. The data are compared to theoretical predictions made with a simple binary diffusion model of partially ionized diatomic gas, namely, nitrogen. Both frozen and equilibrium boundary-layer calculations from this model, as well as equilibrium boundary-layer results from other calculations, are compared to the data. The applicability of frozen and equilibrium calculations are discussed. Although it is not possible to differentiate between a number of the very similar theoretical treatments of this problem from the present data, it is concluded that the transport properties of air up to 15,000°K are known to an accuracy of approximately a factor of 2, and that heat conduction by electrons does not present a serious engineering problem for flight velocities up to 55,000 fps.

Introduction

THE possibility that the great mobility of electrons in highly ionized gases could have the effect of enhancing heat conduction in a boundary layer in such a gas has been an area of considerable research over recent years.[1–3] The lack of conclusive experimental data and the difficulties of calculating and measuring the transport properties of such gases have left this question in a state of uncertainty. Recently, the stagnation point heat transfer in partially ionized air has been the center of considerable controversy. At present there are serious uncertainties in both the available theoretical and experimental results.

The experimental investigation of the stagnation point heat transfer in partially ionized air reported herein was initiated to help answer the questions raised by various theoretical and experimental treatments.[4–9] In order to achieve this purpose the authors felt that a minimum requirement of the scope of the present experiments should be threefold, i.e., 1) a thorough scrutiny of the operation of the shock tube and verification of the existence of a homogeneous hot gas sample of finite length; 2) extension of the velocity range of the experiments to conditions where a dominant fraction of the energy is invested in ionization; and 3) collection of a sufficient quantity of data to allow for meaningful statistical analysis.

Experimentally, the problem of heat transfer in ionized air differs from the lower speed, dissociated air situation in two respects. The first is the problem of creating ionized air of known or calibrated composition in which the measurements are to be made. The second problem arises because the diagnostic techniques which have been developed for heat-transfer measurements have their difficulties when applied to highly conducting gases. The first of these two problems was solved by the development of the electric arc-driven shock tube.[8, 10] Arc-driven shock tubes capable of producing equilibrium degrees of ionization in air as large as 60% have been operated successfully. The other problem has been overcome by improvements in the experimental techniques involved with heat-transfer gages. In this paper we will discuss, first, the verification of the existence of homogeneous gas conditions; secondly, the heat-transfer instrumentation and techniques; and, finally, the experimental heat-transfer results and their import in the light of our present knowledge of the heat-transfer mechanism, transport properties, and associated phenomena.

Shock Tube

The experiments were performed in an electric arc-driven shock tube, 6 in. in diameter and approximately 30 ft long.[10] In this device a strong shock wave is created by the discharge of up to 90,000 joules of electric energy into a light gas confined in the driver section. The discharge creates a longitudinal arc column along the axis of the driver between the electrode and the diaphragm region in which the gas is heated by joule dissipation to a very high temperature. The column expands and the conditions equalize throughout the driver gas, helium in the present experiments, and temperatures of approximately 20,000°K are achieved. As the arc energy is transferred to the gas, the driver pressure rises to a maximum value. A diaphragm separating the driver from the driven or test section bursts at approximately this instant and a strong shock wave propagates down the shock tube.

The operation and performance of this type of shock tube were discussed in detail in Ref. 10. It is common practice to measure the actual shock velocity in each experiment and, consequently, nonideal aspects of the driver operation do not affect the experimental data. However, driver phenomena do limit the highest velocities achievable in this type of shock tube. An important limitation of the present experiments is the loss of ideal test time in such a shock tube. Several phenomena contribute to this loss. The finite time required to open the diaphragm and the probable asymmetries in the diaphragm opening process are two contributors.

Presented at the IAS 31st Annual Meeting, New York, January 21–23, 1963; revision received September 13, 1963. This work was sponsored by the Ballistic Systems Division, Air Force Systems Command, U. S. Air Force, under Contract AF 04(694)-33. The authors would like to acknowledge many fruitful discussions with Nelson Kemp and James Fay, and the able assistance of Charles Saunders, Jr., in the operation of the experimental equipment.

* Principle Research Scientist. Member AIAA.
† Senior Engineer. Member AIAA.

Asymmetries in the energy distribution in the driver also occur. All of these effects introduce disturbances into the driver gas-test gas interface which may grow as the interface proceeds down the shock tube. For high velocity operation, this interface may be unstable because a dense gas is pushing a less dense one in a decelerating system.[49] This Taylor instability helps the turbulence at the interface to grow. Lastly, the boundary layer acts as a path by which the gas in the test slug can escape through the interface.[11] This effect is best seen by considering the mass flow past the interface in an interface-fixed coordinate system. In this frame of reference, the gas immediately adjacent to the wall flows out of the test slug past the interface into the driver gas region at a velocity equal to the velocity of the wall relative to the interface, which is equal to the negative of the flow velocity behind the shock, i.e., $-U_2$.

Measurement of the shock velocity alone is not enough to verify the proper operation of a high performance shock tube. The test time must be carefully observed and monitored for its duration, steadiness, and other characteristics. The test time loss due to the flow of gas past the interface in the boundary layers has been calculated for the present experiments from the theory of Roshko,[11] using boundary-layer calculations for a variable fluid properties model suggested in Ref. 10. The calculated test time duration is compared to the measured performance in Fig. 1. The measured data were obtained by viewing the radiation from the test gas with a collimated photomultiplier having approximately $\frac{1}{2}$ μsec time resolution. The test time was judged as the distance between the onset of radiation in the form of the nonequilibrium overshoot and the increase in radiation when the interface arrives. Samples of the observed radiation profiles are shown in a later section. Although only a fraction of the calculated test time is actually achieved, the observed radiation profile duplicates the ideal picture, i.e., a nonequilibrium overshoot followed by a steady equilibrium region which is terminated by a sudden rise of intensity at the first indication of the arrival of the interface. The enhanced radiation at the interface must be explained as evidence of the presence of driver gas and/or wall or diaphragm impurities in a region which is still predominated by hot test gas. This region lasts approximately 50 μsec, and its intensity varies directly with the peak driver temperature, i.e., the amount of foreign material in the driver gas. The later driver region in which the driver gas dominates the temperature is, of course, quite cold.

The present performance of electric arc-driven shock tubes has allowed simulation of stagnation conditions of flight velocities as high as 55,000 fps. The principle of stagnation

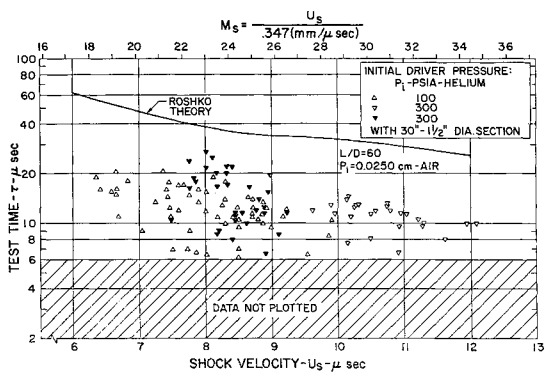

Fig. 1 Time interval between the arrival of the shock front and the first indication of the arrival of the interface as measured from radiation emission. The data are compared to the calculated test time based on the Roshko[11] theory, modified by the boundary-layer corrections of Ref. 10. Note the improvement of the average test time measured after the installation of the 30 ft long, 1½ in. diam section immediately downstream of the diaphragm.

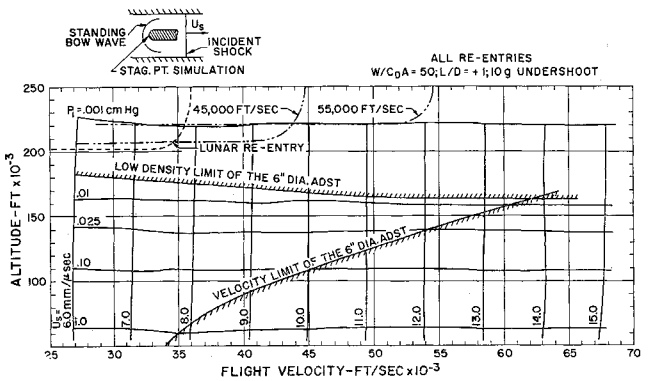

Fig. 2 Stagnation point simulation[12] in a high velocity shock tube. The shock tube conditions, i.e., shock velocity and initial pressure, are plotted on an altitude flight velocity grid at the points where identical stagnation conditions are achieved. The maximum deceleration trajectories of typical lifting re-entry vehicles ($L/D \sim 1.0$) for various entry velocities are shown for reference.

point simulation in shock tubes, and the Mach number independence of stagnation point heat-transfer experiments were discussed in detail in Ref. 12. Figure 2 shows the shock tube operating conditions superimposed on a flight velocity-altitude grid at those points where identical stagnation conditions are produced in the two situations. The present operating range and limits of the 6 in. arc-driven shock tube are also shown. Typical re-entry trajectories for vehicles with an L/D of 1.0 are also included in the figure. The low density limit of a 6 in. shock tube (at high shock velocities) of about 100μ initial pressure misses density simulation of the trajectories by about 1 order of magnitude.

Instrumentation

Shock-tube heat-transfer measurements have been performed mainly by two techniques‡; namely, the thin film resistance thermometer[13] and the thick resistance thermometer or calorimeter.[14] The relative merits of the thin and calorimeter gages were discussed in Refs. 12 and 13. For the present application, the choice was clear. Where high heat-transfer rates are involved, thin gages require that large corrections be made to account for the nonuniform thermal properties of the resistance element and the back-up material as the surface temperature rises significantly.[16] The low resistance of the calorimeter gages make them simpler to insulate from the gas in cases where such insulation is necessary to separate electrically the currents in the gage from the ionized conducting gas. For these reasons, calorimeter gages were used exclusively in the present experiments.

Another advantage of the calorimeter gage is the ability to dispense with gage calibration. In Ref. 14, the properties of chemically pure platinum were checked by dynamic calibrations, and it was concluded that the static bulk material properties were usable in data reduction. This procedure has been followed again in the present experiments, but in view of the unexplained scatter in the data, this choice may not have been too wise.

Heat-transfer gages were mounted at the stagnation point of hemispherical noses of cylindrical models of 0.635 and 1.27 cm radius, by the techniques described in Refs. 12 and 14. The gage elements were either mounted directly on the model surface or were recessed to a depth of their own thickness without any noticeable difference in results.

During the initial experiments erratic signals were observed at the instant the shock passed the gage and fre-

‡ Recently an infrared heat-transfer gage has been developed which holds great promise for this type of measurement in highly conducting gases.[15, 51, 52]

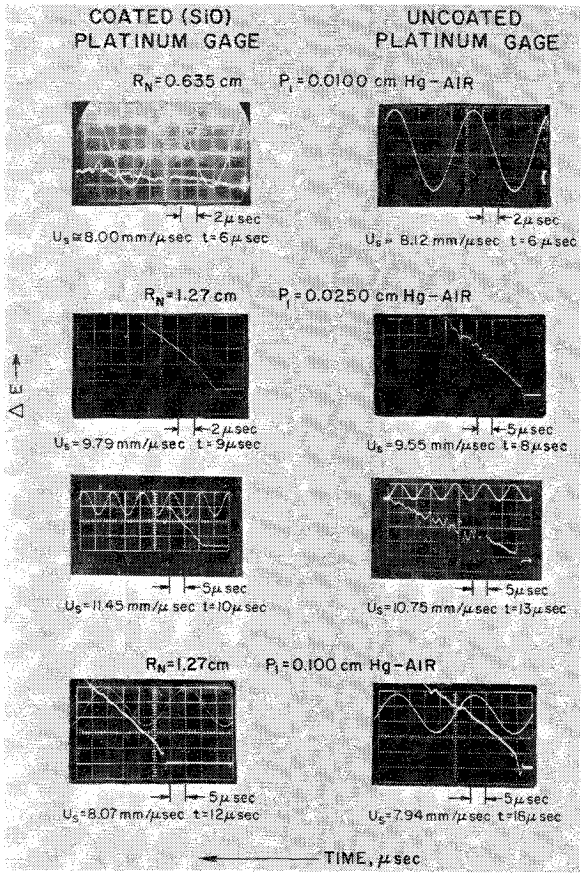

Fig. 3 Oscillograms of heat-transfer records taken with uncoated and coated (Si O) calorimeter gages. After the initial transient, the gage output rises approximately linearly with time characteristic of a steady heat-transfer rate. Data from various shock velocity experiments are shown. Data from the slower shocks are generally of better quality and show longer test time. Maximum and minimum slopes of each oscillogram were measured to estimate the uncertainty of the measured rates. The accuracy of each experiment was considerably better than the run-to-run repeatability.

quently through much of the test time. By careful shielding and proper balancing of the gage and oscilloscope circuit, it was possible to eliminate almost all spurious signals (except the first few microseconds) and to produce repeatable results. This result was observed both when the gages were covered by a thin coating of either silicon-monoxide or silicon-dioxide, approximately 0.1 μ thick. No significant qualitative differences in the data or their absolute value could be detected between coated and uncoated gages except at the highest shock velocities experienced. At shock velocities above 10 mm/μsec, insulating coatings were found to be necessary for obtaining interpretable data. Typical oscillographs from heat-transfer gages taken throughout the velocity range are shown in Fig. 3. The data at the lower velocities are generally of better quality. Equivalent data were obtained by both coated and uncoated gages up to shock velocities of 10 mm/μsec.

Several theoretically predictable effects have been clearly identified in the data. The time required to establish an equilibrium flow geometry about the model[17] is shown in Fig. 4. This time is roughly the time required to traverse one nose radius at the stagnation speed of sound. There was a general trend of shorter transient times for stronger shocks, i.e., the transient became shorter as the sound speed at the stagnation conditions increased. However, the data were too scattered to allow quantitative analysis of this effect.

When thinner gage elements were used, heat loss through the rear face of the element to the model was noticeable. This effect was evidenced by a curvature of the normally linear slope of the calorimeter records. As predicted,[14] platinum gage elements of 0.0007 and 0.0008 in. thick readily showed this effect. Following the analysis of that reference, this effect could be corrected in data reduction. Figure 5 shows data obtained with 0.0007- and 0.0013-in.-thick gages. The correction for heat loss to the backing brings the nonlinear response from the thinner gage elements close to linear, whereas the thicker element is not affected by the correction. If the gage element is made too thick, the heat does not penetrate the gage in the test time and the temperature distribution in the gage becomes highly nonlinear. The analysis of calorimeter data assumes a linear temperature distribution in the gage element. A second-order correction term can be written[14] for this effect but is negligible for the present experiments.

The reproducibility of the data presented is not as good as one might hope for from this type of data. The largest error appears to be introduced by gage uncertainties, particularly the difficulty of knowing the precise value of the resistance corresponding to the effective gage area and the contact resistance of the connections to the gage element. Measured gage resistances of approximately plus or minus 15% of the value computed from the handbook resistance and the assumed effective gage dimensions were common. The difficulty is one of obtaining a voltage change measurement which is entirely due to only the resistance element which is sensitive to the heat pulse. If the gage resistance measurement includes any resistance other than that of the effective gage element undergoing the resistance change due to the calorimeter effect, this difference will appear to be an increment in heat transfer in the data. It is possible that dynamic calibration could have improved this situation.

All other measurements were made with far greater accuracy. The initial pressure was measured by both an alphatron and McLeod gage and the velocity by the output from

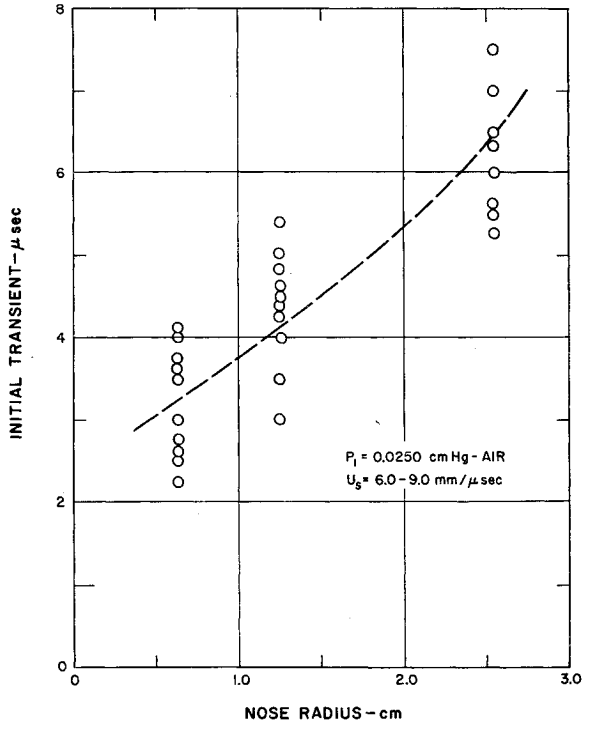

Fig. 4 Time required to establish steady flow about the heat-transfer models. The time duration of the initial electrical transient is shorter than the time at which the initial curvature of the oscillogram terminated. This point is assumed to indicate the time at which the boundary layer and the shock curvature (i.e., stagnation-point velocity gradient) achieve a steady geometrical configuration.[17]

a number of upstream side-wall heat-transfer detectors, both to better than 3% accuracy. Immediately in front of the model the shock velocity was measured again by three photomultipliers, this time to better than 2% accuracy. In data reduction the shock velocity was extrapolated to the gage location. The output of the heat-transfer gages was recorded on Tektronix 535 oscilloscopes with differential preamplifiers, 53/54*D*. A Ballentine voltage standard was recorded on the oscillogram for every experiment. It must thus be assumed that the conditions of the flow were known accurately in every experiment, and that the measurements were taken with sufficient accuracy to produce data with a maximum deviation of less than 10%. The balance of the scatter of the data must be attributed to the gage uncertainties.

Auxiliary Measurements

The measurements were obtained at initial shock tube pressures of 1 and 0.25 mm, and shock velocities of 6 to 12 mm/μsec. For each experiment, measurements were made to verify the proper operation of the shock tube while the heat-transfer measurement was being made. This appears as an extreme measure compared to standard shock-tube techniques, but it has been our experience that the operation of shock tubes under these extreme conditions is occasionally erratic, and such verification is essential to prevent misleading results.

The standard auxiliary measurement made for every experiment was the radiation profile taken with photomultipliers viewing across the shock tube. Time resolution of about $\frac{1}{2}$ μsec was obtained through the use of collimated narrow slits. Proper operation of the shock tube was judged by the appearance of a nonequilibrium overshoot of the proper width and intensity,[18] followed by an approximately steady radiation level indicative of the equilibrium region in the test gas. The test is considered terminated when the first evidence of the interface is seen as previously discussed. A selection of typical radiation histories is shown in Fig. 6.

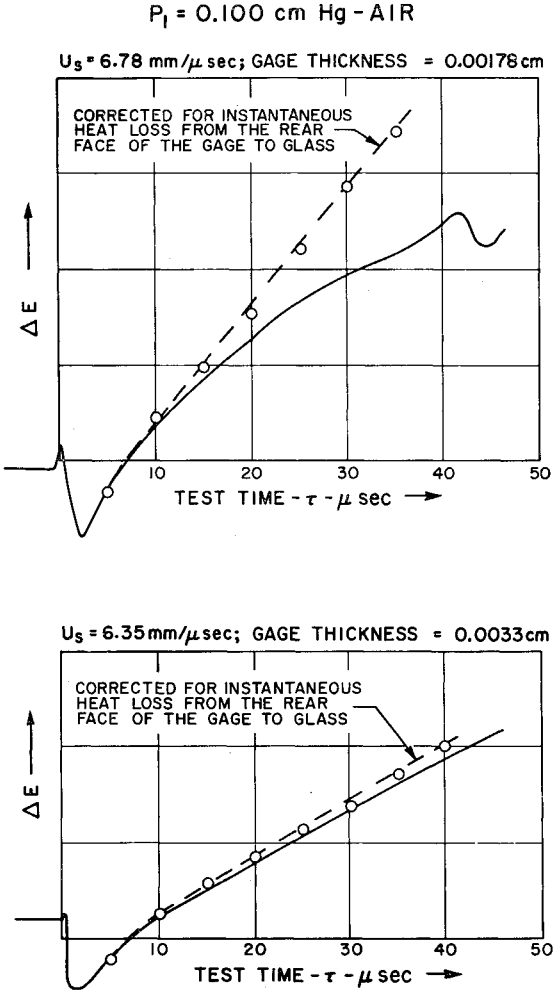

Fig. 5 Correction of heat-transfer gage output for the heat loss through the rear surface of the gage.[12] Corrections are shown for a gage which is too thin and one which is of the proper thickness for the experimental conditions.

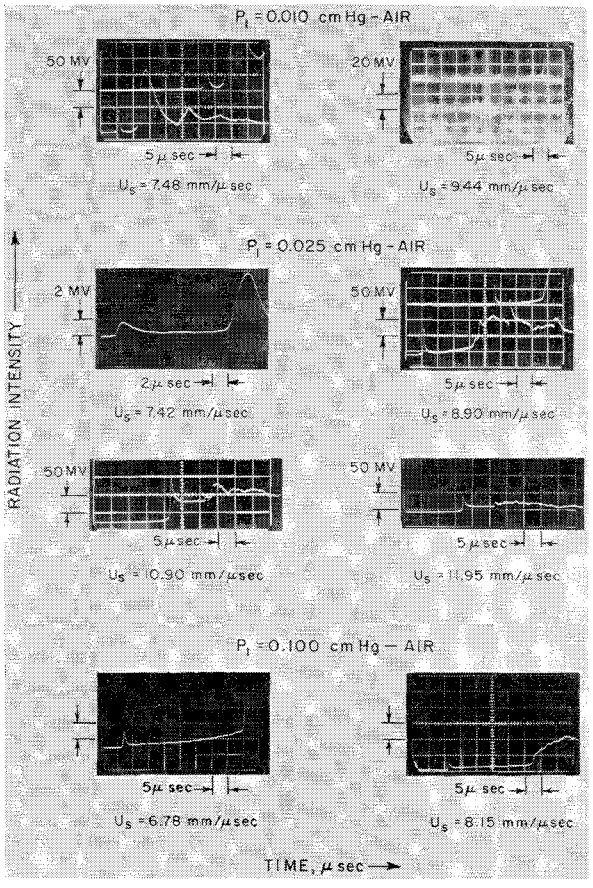

Fig. 6 Profiles of visible radiation emission in the 0.4–0.6μ wavelength region. The radiation profiles were recorded by a photomultiplier viewing through a set of collimated slits across the shock tube. Profiles show the radiation history behind the incident shock, i.e., the nonequilibrium region, the steady equilibrium zone, and finally strong emission from the interface. Intense interface radiation is typical of arc-driven shock tubes and can be adjusted by altering the driver conditions. This excess radiation lasts for approximately 50 μsec.

Two other measurements have been made, however, on a more sporadic basis. Image converter pictures were used to visualize the whole test gas due to its luminosity, and a photomultiplier was used to observe the radiation from the inviscid flow field behind the bow shock in the stagnation region. The image converter gives a vivid view of the state of the test gases. The nonequilibrium shock front, steady equilibrium region, and interface are clearly visible. The interface is seen to be a region of large scale, nonaxial motion, i.e., turbulence, even in experiments where considerable test time is clearly visible. The test time correlates with, but is always less than, the test time predicted in Ref. 10. Turbulent mixing at the interface probably accounts for this departure from the theory. The violence of this turbulence determines what fraction of the calculated test time is actually achieved. There is no apparent systematic difference between experiments which show a finite test time and those in which the interface turbulence is sufficient to consume all the test gas. Examples of image converter data,

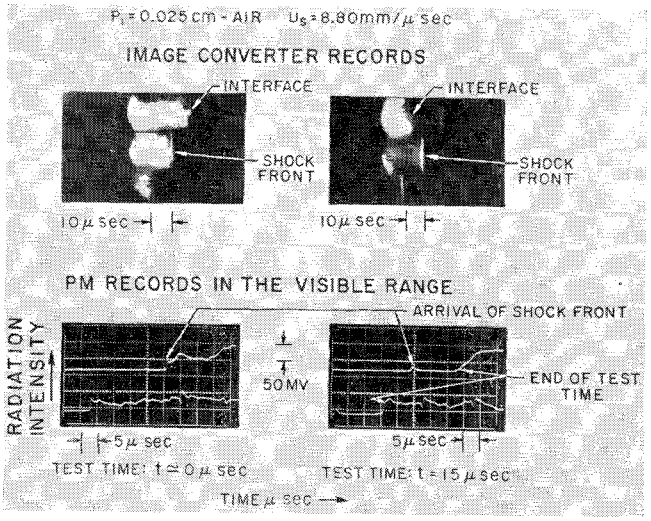

Fig. 7 Instantaneous photographs of the shock-heated air and driver gas taken with an image converter (STL Model C). There are three 0.05 μsec exposures in each picture taken at 10 μsec intervals. Right-hand picture shows a properly developed hot gas test slug followed by a turbulent interface. Left-hand picture shows the interface and shock front unresolved representative of a run during which no test gas has accumulated.

together with corresponding photomultiplier records, are shown in Fig. 7 for two experiments, one in which a finite test time is visible and one in which there is no test time.

The other measurements involved looking at the radiation emanating from the inviscid flow region between the bow shock and the body at the stagnation point. A photomultiplier viewed a point in the flow $\frac{1}{2}$ mm in front of the stagnation point through a set of vertical collimated slits approximately $\frac{1}{2}$ mm wide. For a 1.27 cm radius model, the standoff distance of the shock at the stagnation point is approximately 2 mm. A careful examination of the oscillograph records from this measurement shows a number of phenomena which verify the proper operation of the shock tube. When the incident shock passes the field of view of the slit, a small but very steep rise can be seen. The shock reflected from the model comes into view after a fraction of a microsecond and the radiation intensity rises by about an order of magnitude. The initial fast rise becomes more gradual in this region, lasting about 5 μsec. We attribute this to the time required for the bow shock geometry in the field of view of the photomultiplier to reach its final configuration. This process should require slightly more time than the boundary-layer transient shown in Fig. 4. Following the rise, an approximately steady radiation intensity is seen until the interface arrives. These characteristics are visible in the sample oscillograms shown in Fig. 8.

A time-resolving drum camera spectrograph with f 4 optics was set up to view the inviscid flow in front of the stagnation point in a small number of experiments. Although no high quality spectra were taken, it was clearly evident that no non-air sources of radiation were visible during the 15–20 μsec test time except the hydrogen Balmer series. The air-nitrogen band structure[19] was identifiable. These aspects of the performance of arc-driven shock tubes have also been documented thoroughly in Ref. 10.

State of Test Gas

Having established the existence of a homogeneous gas sample under the experimental conditions, it remains to determine the thermochemical state of the test gas. In this determination, three regions are involved, i.e., the gas behind the incident shock, the stagnation region, and the boundary layer. All three regions must be considered from the point of view of dissociation and ionization equilibration.

The state of the dissociation processes can be established from the extensive available literature of the chemical kinetics of air.[20] Behind strong normal shock waves, the distance or time required by a flow to relax to a thermodynamic equilibrium state can be calculated from the rates summarized by Wray.[20] The observations of Allen, et al.,[18] of the time required for the radiation from the molecular bands of nitrogen to return to the equilibrium level after the initial overshoot at the shock front are a measure of this equilibration time (or distance), and can be applied to the present experiments. Figure 9 shows these results calculated for the conditions of this experiment. The corresponding data observed from the photomultiplier viewing across the shock tube are also shown. The measurements generally agree with the interpretation of Allen's data except at the high shock velocities where the nonequilibrium region was not resolved. It can be concluded that at initial shock-tube pressures of 0.25 mm and higher, and test times of 6 μsec and more, almost all of the incident gas is in dissociation equilibrium, except possibly at the lowest shock velocities where test times are considerably longer.

The relaxation process in the gas behind the standing or bow shock wave in front of the model is another aspect of the same question. Due to the much higher temperatures, the relaxation is considerably faster, but the characteristic length, in this case the shock detachment distance, is also much smaller. The time or distance required for the dissociation process to equilibrate in this gas can be estimated by extrapolating the data of Allen[18] and by application of shock mapping.[48] The resulting distances required by the air to equilibrate behind the standing or bow shock are shown in Fig. 10. Also shown are the shock detachment distances for two model sizes used in this experiment. The equilibra-

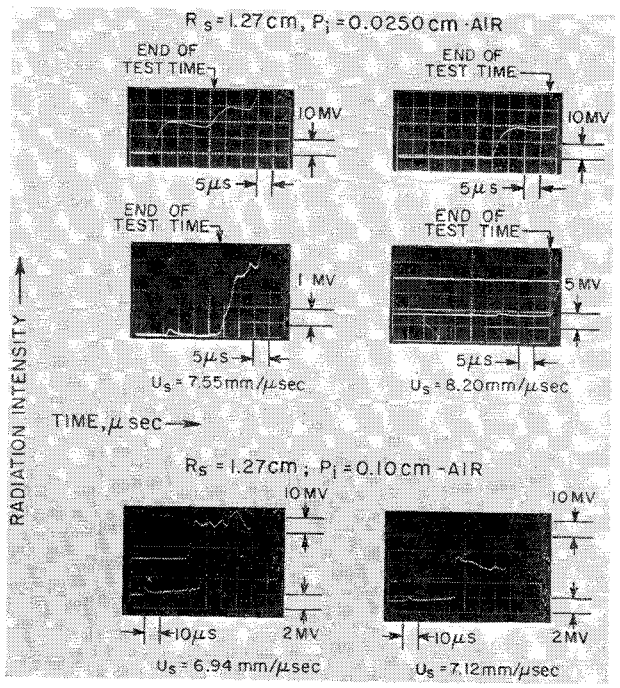

Fig. 8 Radiation emitted from the inviscid flow behind the bow shock of a heat-transfer model. The photomultiplier viewed a vertical slit ½ mm wide, whereas the shock detachment distance was approximately 2 mm, and thus sees the gas in front of the stagnation point. The slight, fast initial rise is interpreted as the passage of the incident shock before it reaches the model. The slower rise to the equilibrium level is interpreted to be due to the time required by the flow geometry to establish its equilibrium configuration (see Fig. 4). The second rise corresponds to the arrival of the interface as also seen in the incident shock radiation (see Fig. 6). Upper Trace: *PM* at stagnation point of hemisphere-cylinder model; lower trace: *PM* 20 cm ahead of model.

tion distances are seen to be equal to, or smaller than, the stand-off distance over most of the experimental range. Only the low shock velocity, 0.25 mm initial pressure experiments can be in some doubt. The estimate based on the definition of equilibrium as the point where radiation intensity has relaxed to only 10% above the equilibrium level is very conservative in the present context of determining the departure from equilibrium. Also, in a two-shock process, i.e., where half the enthalpy is added across the incident shock and half across the bow shock, equilibration across the second shock is probably faster because of the population of excited energy level in the incident gases. The estimate is uncertain because the data of Ref. 18 were extrapolated by about 50% in velocity. These considerations are the basis for our contention that the dissociation process was in equilibrium at the edge of the boundary layer throughout the present experiments.

The final consideration of the equilibration of the dissociation process concerns the state of the gas in the boundary layer. The conditions under which a boundary layer will be in equilibrium, frozen, and in some intermediate state, were determined by Fay and Riddell's numerical solutions for a reacting stagnation point boundary layer.[21] In this reference a parameter C_1 is proposed to measure the state of recombination in the boundary layer as follows:

$$C_1 = K_1(P_s/R)^2\, T_s^{-3.5}(dUe/dx)^{-1}$$

where $K_1T^{-1.5}$ was derived from the oxygen recombination rate and its temperature dependence,[22] P_s is the stagnation pressure, T_s is the stagnation temperature, R is the universal gas constant, and dUe/dx is the velocity gradient at the stagnation point. C_1 is essentially the ratio of the oxygen three-body recombination time to the flow time of a particle in the boundary layer. It was shown that when this parameter

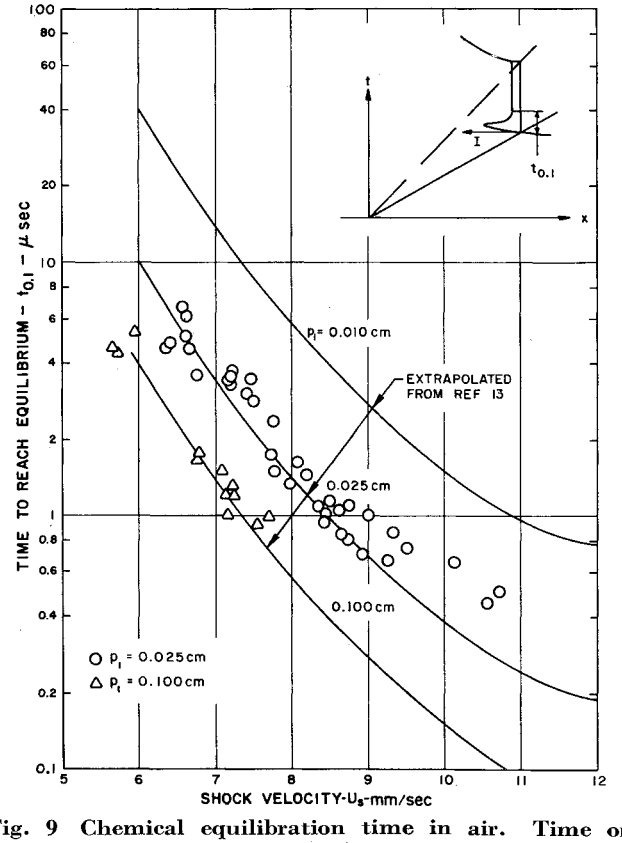

Fig. 9 Chemical equilibration time in air. Time or distance behind a normal shock at which the radiation from the nitrogen molecule band systems will decay to within 10% of the equilibrium value. Times were calculated from data of Ref. 18 and data points were observed in present experiments, i.e., Fig. 6. Limit of time resolution of present data is approximately ½ μsec.

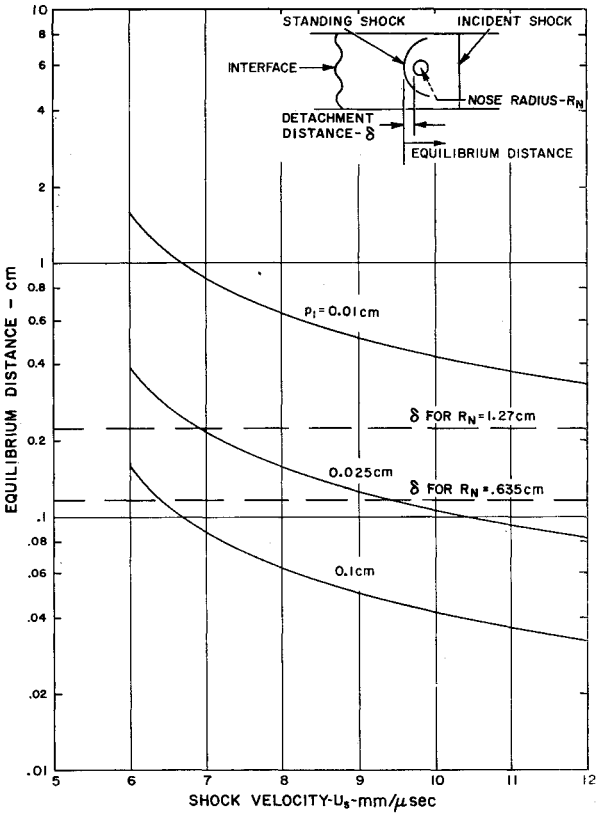

Fig. 10 Chemical equilibration distance behind standing shock. The distances shown were calculated by extrapolation of the data of Ref. 18 to 50% higher velocities and shock mapping as discussed by Gibson.[18] This estimate is felt to be conservative because the gas ahead of the standing shock is already partially dissociated, and equilibration from this condition should be faster than starting from cold gas.

reaches a value of 1, the boundary layer starts to freeze. However, a value of 10^{-4} is required before the freezing is sufficient to affect the heat transfer strongly, i.e., a recombination parameter of less than 10^{-4} is required before the effects of the catalytic efficiency of the surface can affect the heat-transfer measurement. Thus, equilibrium boundary calculations should be valid for $C_1 > 1.0$, frozen boundary-layer calculations for $C_1 < 1.0$. However, for surface effects to be a possible source of differing heat transfer measurements, a value of $C_1 < 10^{-4}$ is required. The foregoing results were shown to be valid for a wide range of flow conditions and surface temperatures by Goodwin and Chung.[23]

In our evaluation of the parameter C_1 the room temperature recombination coefficient for oxygen atoms was taken to be 1.0×10^{15} cm^6/mole^2-sec from a recent review of the available data.[24] It is now known that the temperature dependence of the oxygen recombination process is much weaker than $T^{-3/2}$, or in fact, $T^{-1/2}$, or is even nonexistent.[25] This lesser temperature dependence will change the calculation of the point of onset of boundary-layer freezing. The form of the recombination coefficient suggested by Goodwin and Chung[23] has allowed Inger[26] to propose a correlation which accounts both for variations of the temperature dependence of the recombination rate coefficient and the wall or surface temperature as follows:

$$C_1 = K_1T^{\omega}(P_s/RT_s)^2(dUe/dx)^{-1}$$

where ω is the temperature dependence exponent of the recombination rate just discussed. The recombination parameter calculated from the foregoing equation is shown in Fig. 11. The velocity dependence is very weak, and a single line suffices for the range of this experiment. The value of the coefficient C_1 was below unity for all the experiments

but was not low enough so that surface effects could be measurable in terms of heat-transfer differences.

Much less evidence is available to ascertain the state of the ionization equilibration. Shock tube measurements of the ionization rate for air have been made by Lin and Fyfe[27] at shock velocities up to 7 mm/μsec. The experimental results are in agreement with the complex system of reactions and rates proposed by Lin and Teare.[28] This work indicated that the atom-atom reactions dominated the ionization process in the experiments. The calculations show this condition to exist up to shock velocities of 9 mm/μsec. At this shock velocity it is expected that the electron impact process will become fast enough to dominate the ionization rate, and extrapolations of the data of Lin would not be meaningful. There is also some question about the impact ionization mechanism stipulated by Lin. Lin considers direct, one-step ionization from the ground state only. However, ionization can proceed via the upper levels and such a process can be considerably faster. Thus, electron impact may become important at even lower shock velocities than calculated in Ref. 28. Keeping these uncertainties in mind, the ionization distances behind the incident shock calculated from the mechanism proposed by Lin are shown in Fig. 12. The times required are all considerably less than the test time, and appear to decrease with increasing shock speeds. It is noteworthy to observe that the degree of ionization reaches the equilibrium value early in the relaxation process in the shock front, about the time of the NO concentrations peak, and does not overshoot strongly. Consequently, near equilibrium ionization exists often before recombination is complete in a shock front.

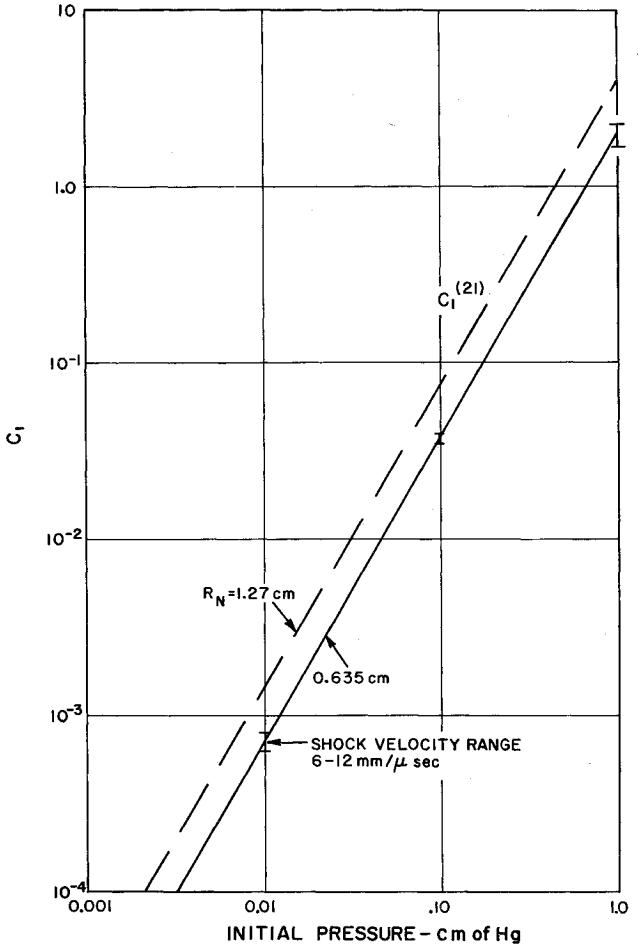

Fig. 11 State of dissociation equilibrium in the boundary layer. The parameter C_1 is the ratio of the recombination time for oxygen atoms to the diffusion time across the boundary layer, as defined in Ref. 21.

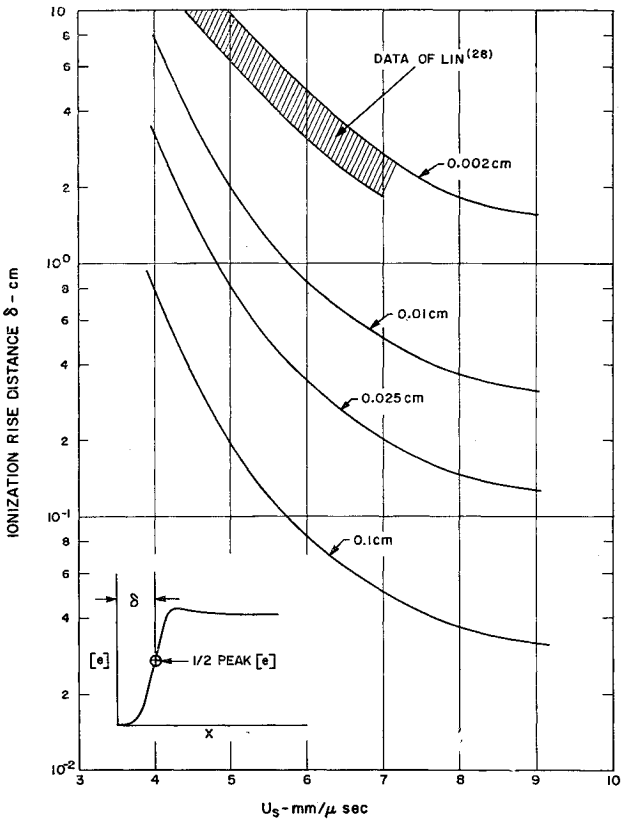

Fig. 12 Estimate of ionization distance or time behind a normal shock. Distance defined as the distance required to reach 50% of the peak electron concentration, from the data of Lin.[28] Region in which experiments were performed and agree with the theoretical model is shown. Other conditions are achieved by scaling the calculations.

Behind stronger incident shocks, uncertainties exist about the dominant process. The atom-atom process is already very fast in shock fronts of 9 mm/μsec. A process would have to be even faster to dominate the over-all ionization rate. This argument leads to some assurance that ionization equilibrium should exist behind the incident shock. In opposition to this argument is the fact that the strongest shock calculation made for the Lin model considers equilibrium ionization levels of only fractions of 1%. At the fastest shock velocities of this experiment about 20% ionization exists behind the incident shock in equilibrium. Consequently, ionization must proceed at considerably faster rates for the process to be complete in the same time, distance, or number of collisions. The foregoing argument admits the possibility that the total ionization distance may become longer at higher shock velocities. The state of ionization behind strong incident shocks is thus still uncertain at this time. The state of ionization in the inviscid flow, i.e., the conditions at the edge of the boundary layer, suffers from these same uncertainties.

The last equilibration question to be treated is the question of electron recombination in the boundary layer. Assuming complete thermodynamic equilibrium at the edge of the boundary layer, we can again resort to interpreting and extrapolating the work of Lin.[28] Electrons can be removed from a hot gas by the inverse of the atom-atom collision processes, i.e.,

$$N + N \rightleftarrows N_2^+ + e$$

$$N + O \rightleftarrows NO^+ + e$$

and by the inverse of the electron impact process, i.e., electron-ion three-body recombination:

$$N + e \rightleftarrows N^+ + e + e$$

The experiments of Ref. 27 give a basis for estimating the maximum rate of removal of electrons at outer edge of the boundary layer for the first of these processes. These data were shown to be explainable by a recombination coefficient for both the N_2^+ and NO^+ processes of $k_R \cong 3 \times 10^{-3}\, T^{-3/2}$. The maximum rate of change of number of electrons for a displacement from equilibrium occurs when the forward reactions are zero, and, thus,

$$d[e]/dt_{\max} = -k_R\,[e][N_2^+ + NO^+]$$

Substituting the recombination coefficient just given,

$$d\ln[e]/dt = -3 \times 10^{-3}\, T^{-3/2}[N_2^+ + NO^+]$$

and the characteristic time for the electron concentration to deplete by a factor of e is

$$\Delta t = \frac{T^{3/2}}{3 \times 10^{-3}[N_2^+ + NO^+]} = \tau_{1\ \mathrm{ion}}$$

A flow time can be defined as the time required by a particle to flow a distance equal to the nose radius, and thus also the time for a particle to diffuse through the boundary layer at the stagnation point.[21] In a Newtonian flow,

$$(dUe/dx)^{-1} \cong R(\rho_s/2P_s)^{1/2} = \tau\ \mathrm{flow}$$

The ratio of the foregoing two flow times is plotted in Fig. 13 for the experimental stagnation conditions. Note that because the equilibrium concentration of N_2^+ and NO^+ becomes very small for strong shocks, electron recombination due to this mechanism becomes very slow. In fact, if this were the only mechanism for removal of electrons, the electron recombination in the boundary layer would freeze at high shock velocities.

The electron three-body recombination process will compete with the previous reactions for removal of electrons at high temperatures. For this reaction we can write

$$d[e]/dt = k_F[N][e] - k_R[N^+][e]^2$$

At equilibrium the forward and backward rates are exactly equal, and, consequently, we can use either one to estimate the maximum possible depletion rate. Using the forward process, we get $d\ln[e]/dt = [N]\,k_F$.

In studying the forward process in a shock front, Lin argued that ionization should proceed from the ground state and that ionization from the excited upper levels need not be considered. On this basis, by estimating the collision cross section, he arrived at the following rate for the forward process:

$$k_F \cong 0.55 \times 10^{-10}\, e^{-169{,}000/T}\, T^{1/2}$$

Giving the characteristic time for this process as

$$\Delta t = \frac{1.82 \times 10^{10}}{[N]} \frac{1}{e^{-169{,}000/T}\, T^{1/2}} = \tau_{2\ \mathrm{ion}}$$

The ratio of this time to the flow time is also shown in Fig. 13.

For a recombination process starting from a high temperature equilibrium state, it is likely that the populated upper excited levels will accelerate mechanism by allowing transition between closely spaced levels to become recombinations by subsequent cascading to the ground state. This mechanism was considered by Bates.[29] He called this process collisional-radiative recombination, and the coefficients for hydrogen are tabulated in this reference. It is further stated that the collisional-radiative decay is not very sensitive to the species of singly charged atoms. Using the tabulated values, a third ion relaxation time $\tau_{3\mathrm{ion}}$ can be calculated. This time is much shorter than $\tau_{2\mathrm{ion}}$ and would take over as the dominant recombination mechanism so that electronic equilibrium will be maintained in the boundary layer throughout the range of the present experiments.

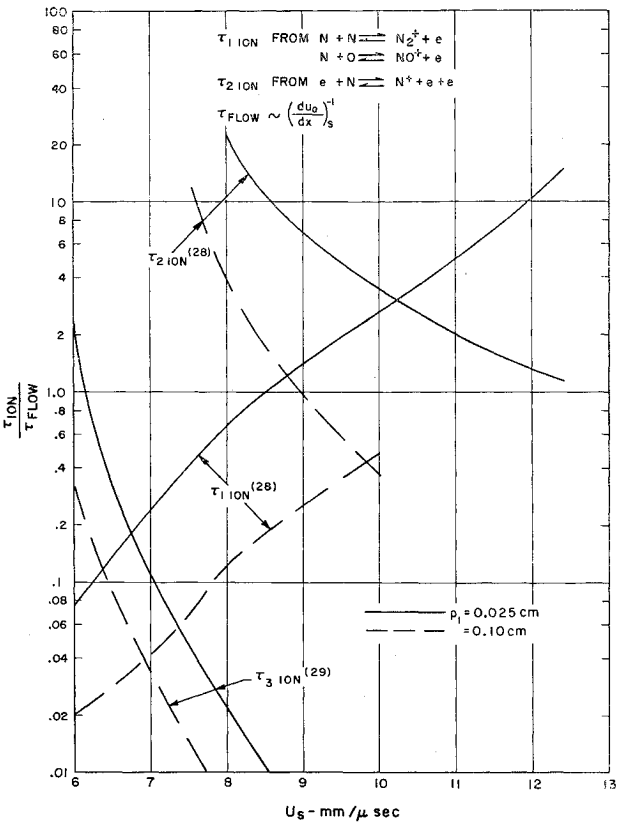

Fig. 13 Estimate of recombination of electrons in the boundary layer, $\tau_{1\ \mathrm{ion}}$ for two-body recombination with molecular ions is slow at high shock velocity because of the small concentration of molecular ions. $\tau_{2\ \mathrm{ion}}$ estimates from Ref. 28 and $\tau_{3\ \mathrm{ion}}$ from Ref. 29 probably bracket the actual rates.

The conclusion which has been tentatively drawn from these considerations of the electronic equilibration is that, in all likelihood, the flow will equilibrate in the boundary layer. The state of knowledge of the ionization mechanism at high temperatures is not sufficient at this time to allow any such statements to be made with great confidence.

Heat-Transfer Results

The heat-transfer data deduced from the present series of experiments are shown in Fig. 14. Only data points from experiments during which at least 6 μsec of test time were clearly verified by one of the methods described have been used. This restriction has separated out the apparent scatter which would be introduced by analyzing data before the initial transient had subsided (see Fig. 4). Data were taken at two initial shock tube pressures, 1.0 and 0.25 mm of Hg of air, simulating flight at altitudes of approximately 110,000 and 140,000 ft, respectively. A shock velocity range reaching a simulated velocity of 55,000 fps has been covered.

Heat-transfer data were obtained with and without thin silicon monoxide coatings. In many cases the uncoated gages were the same physical gages on the second run after the coating had been eroded away. Gages were polished between experiments to remove any residue of the coatings for uncoated gage experiments. Although silicon monoxide and platinum have vastly different catalytic efficiency[30] for atom recombination, no difference in heat transfer is to be expected, as discussed in the previous section. The average values of the data from coated and uncoated gages varied by only several percent.

The data are compared with the results calculated by the Fay and Kemp binary diffusion model for ionized diatomic gases.[31] Both equilibrium and frozen boundary-layer calculations for nitrogen are shown for comparison with the data.

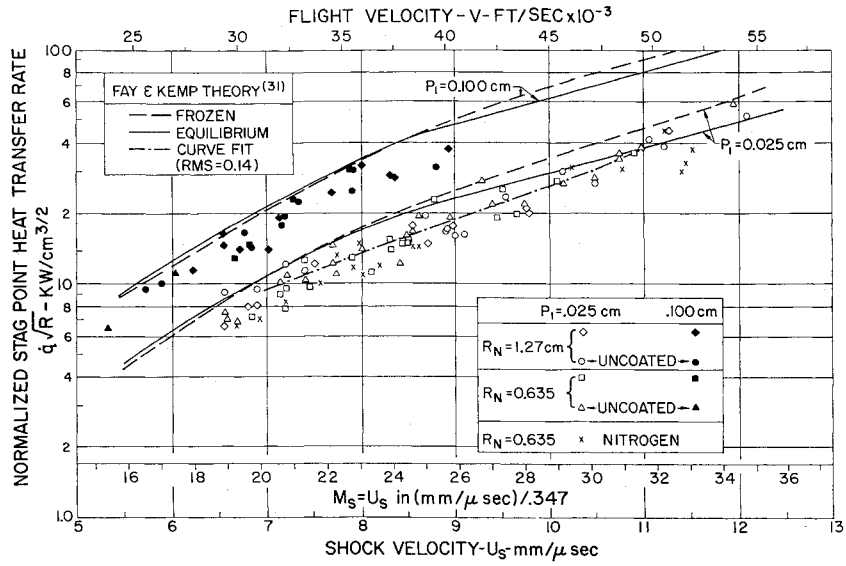

Fig. 14 Measured stagnation point heat-transfer rates. Lines shown for comparison are the results of the calculations for the binary diffusion model for nitrogen at the appropriate conditions, from Fay and Kemp,[31] both for a frozen and equilibrium boundary layer.

The data appear to follow the theoretical predictions in a general way. A curve fit has been made to the data as shown in Fig. 14. The root-mean-square deviation of the data from this curve is 0.14.

The most striking aspect of the comparison between the experiments and theory is the disagreement in the intermediate velocity range. The mean of the experimental points lies approximately 20% below the theories in the 7 to 8 mm/μsec velocity range. A number of effects have been considered to explain this discrepancy.

The possibility that the gas at the edge of the boundary layer was not in equilibrium and that this would in turn affect the heat transfer was investigated. Calculations were performed for cases in which the gas was not allowed to ionize, i.e., ionization was frozen. The ionization energy was redistributed and thus a much greater temperature resulted. However, as has been experienced in other heat-transfer problems in the past, the heat-transfer rates were found to be essentially independent of the division of the energy among the various modes and dependent mainly on the total energy. Consequently, lack of ionization equilibration is not felt to be a cause for the difference.

It has been suggested by Fenster and Rozycki[45] that the differences are due to differences between nitrogen and air. In support of their argument, they point to several effects which could contribute to the phenomena in question. First, Ref. 45 points out that Fenster and Heyman[46] have found that the diffusion of energy at the wall is dominated by the oxygen dissociation energy which is only about half the values of the nitrogen dissociation energy. Inclusion of this distinction in a theoretical calculation has resulted in heat-transfer rates in dissociated air approximately 30% less than calculated from Fay and Riddell. However, Kemp has pointed out that the additional terms considered by Fenster and Heyman to account for the oxygen dissociation energy are only a partial inclusion of the effects due to the diatomic nature of air, and other effects probably of equal significance as those considered, were discounted. This result must be considered as inconclusive at this time.

To treat the ionized air case, Fenster and Rozycki used the transport properties of Peng and Pindroh.[47] Comparing the total conductivity of Ref. 47 with those of Yos[39] and those of Hansen,[38] significant differences are seen to exist. The assumptions, cross sections, and methods used vary too much to identify the source of these differences.

Yos[39] has, however, calculated the transport properties of air and nitrogen by the same method. The result is that the differences between air and nitrogen in general are small. There are, of course, some significant differences. The total conductivity of air is somewhat larger (a factor of 2) in 3000°–4000°K due to the recombination energy of NO. However at about 7000°–8000°K, nitrogen has a higher equilibrium conductivity by about 30%. It should be noted that this region is almost exactly where the heat-transfer rates measured in air are significantly lower than the nitrogen theory. The air thermal conductivity of Yos[39] and Peng and Pindroh[47] agree very well in this temperature range. At higher temperatures the differences between nitrogen and air are negligible according to Yos.§ Thus, at very high speeds one would expect the nitrogen theory to be a better approximation for air than it was at lower speeds.

In order to further validate the use of a nitrogen theory for air, a number of experiments were performed in nitrogen. These data are shown in Fig. 14 as crosses. As expected, the agreement of the mean of these data with the air values in the high shock velocity range was quite satisfactory. However, in the 7–8 mm/μsec shock velocity range, where the air conductivity according to Yos is lower, the nitrogen and air data also agree. Thus, the measured nitrogen heat-transfer rates were also some 20% less than predicted by the theory. Arguments based on the differences between air and nitrogen must consider these data. The use of the binary diffusion nitrogen model as a basis for comparison of theory and air experiments appears justified, but all questions are still not completely settled.

The possibility of the Lewis number being lower than the assumed value was also considered. The theory for a frozen boundary layer with Lewis number approximately 0.3 appears to follow the experimental data quite reasonably. However, it has not been possible to devise a reasonable argument on why the Lewis number should have such a small value.

Finally, the applicability of any boundary-layer theory in which all constituents have the same temperature must be questioned. At present, no boundary-layer theories which allow variations of the electron temperatures exist. This question appears to be a fruitful area of future research.

The factor of 2 difference between the heat transfer from the equilibrium and frozen boundary-layer calculations at 60,000 fps is a striking result of Ref. 31, which emphasizes the importance of knowing the precise thermodynamic state of the gases at the edge of the boundary layer. In the dissociated boundary-layer case, the total heat transfer could only be affected by extreme freezing, $C_l < 10^{-4}$, in combination with noncatalysity of the surface. In the ionized case, no surface effects were considered or were needed to alter the heat transfer. Thus, the forementioned difference is a new phenomenon and should be understood. The present

§ Reference 47 calculates the conductivity of air to be considerably greater than the nitrogen values calculated by Yos.

experimental data are not capable of differentiating between the two models. The experiments were performed under assumed equilibrium or near equilibrium conditions, and the measured heat-transfer rates appear to be depressed below the frozen calculations. An experiment specifically designed to detect the presence of ions and electrons at the bottom of the boundary layer would be valuable in differentiating between these two models, because these particles exist near the wall only in the frozen boundary layer.[31]

An estimate was made of the magnitude of the contribution to the measured heat transfer which could be attributed to radiative heating. Radiation data for air at the temperature, density, and degree of ionization which are encountered in this experiment are not very complete. The various existing radiation calculations and tables[33–35] are either based on data obtained at lower temperatures or are purely theoretical calculations. Their results differ by a factor of 2 at the experimental conditions of this study. An analysis of the differences between these tables has been made by Keck.[36] He concluded that calculations based on emission measurements are preferable to those derived from theoretical calculations of high temperature emission from discharge or absorption measurements at room temperature. The only emission data obtained applicable to the experimental conditions are the preliminary measurements reported in Ref. 37. As these data have not yet found their way into a complete radiation calculation, the work of Kivel[33] has been utilized in this study for estimating radiation. These calculations agree within a factor of 2 with the other available tables.[34, 35]

The ratio of the equilibrium radiative heating rate to convective heating rates calculated from these data is shown in Fig. 15. The largest value of this ratio encountered was 0.3, which occurred at the maximum velocity and dropped very rapidly with shock velocity. In view of the fact that the gage material certainly does not absorb all of the incident radiation as assumed in the calculation, and that the results of Ref. 37 appear to indicate that the radiation predicted by Kivel may be high by a factor of about 2 in this temperature region, no effort was made to apply this result as a correction.

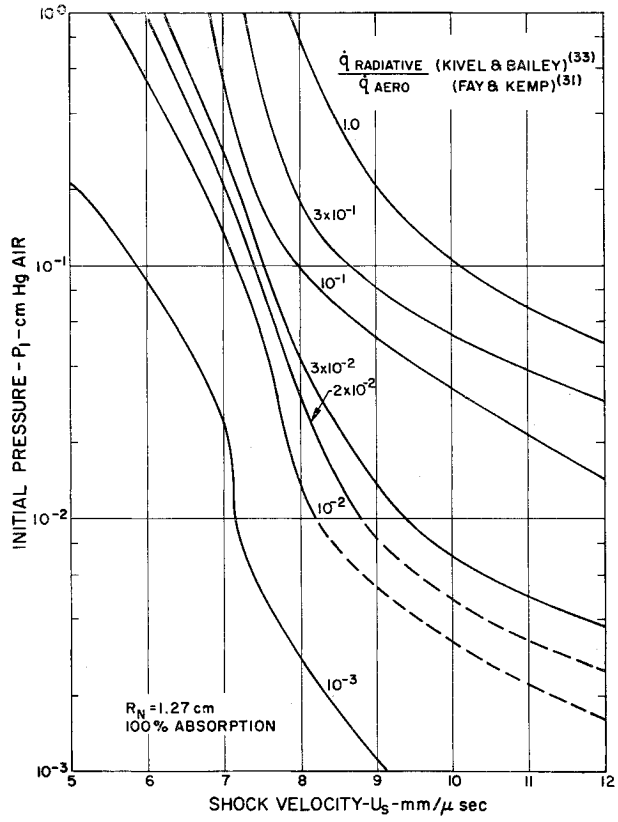

Fig. 15 Ratio of radiative and convective heating at the stagnation point of models used in the present experiments. Convective heating was calculated from Fay and Kemp,[31] equilibrium boundary layer and radiative heating was calculated from Kivel and Bailey,[33] assuming 100% absorption by the gage. Indications are that Ref. 33 overestimates the radiation by approximately a factor of 2. The ratio scales as the nose radius to the three-half power.

One other source of radiation was considered but discarded. It has been noted that the driver gas radiates quite intensely (see Fig. 6). This radiation is incident on the gage even before the shock arrives at the gage and the aerodynamic heating occurs. The strength of the source of this radiation varies only slowly as the shock wave proceeds down the shocktube as the solid angle subtended at the gage changes. During the interval between the time when the incident shock is about 1 tube diameter upstream of the gage and the time the interface arrives to this point, the solid angle viewed by the gage changes by a factor of about 3. Thus, if this source produced significant heating at any time during the experiment, it should also be visible before the arrival of the incident shock front. No such signal has ever been detected by heat-transfer gages.

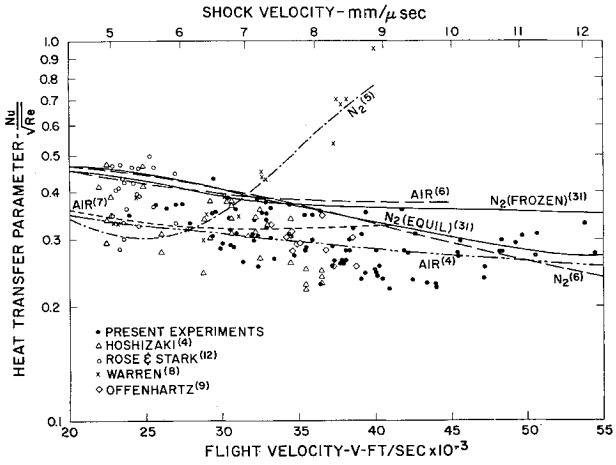

Fig. 16 Summary plot of various experimental data and theories for stagnation point heat transfer in partially ionized air and nitrogen. Pallone's,[6] Hoshizaki's,[4] and Cohen's[7] theories are shown applicable to a stagnation pressure of 1 atm. Fay and Kemp[31] was calculated for the experimental conditions, i.e., $p_1 = 0.025$ a.u. of Hg. Scala[5] was calculated for a flight altitude of 240,000 ft.

Comparison with Other Theories and Experiments

Figure 16 shows a summary of the theories and data on heat transfer in partially ionized air and nitrogen known to the authors. The stagnation-point heat-transfer rates calculated from the theories of Hoshizaki,[4] Pallone,[6] Cohen,[7] and Fay and Kemp,[31] agree within plus or minus 25% up to velocities of 55,000 fps. Note that the calculations of Hoshizaki, Cohen, and Pallone for air all used the transport properties of Hansen[38] and are essentially equivalent analyses.‖ The difference between their results must thus be attributed to numerical differences and to the particular correlation equations proposed by the authors for their numerical results.

Pallone[6] has used the transport property calculations of Yos[39] for his calculations for nitrogen. These calculations may be compared directly with the work of Scala.[5] Scala's

‖ Pallone recently has used the transport properties of Yos [39] for air with results indistinguishable from his nitrogen curve.

calculation is for a four-component mixture of nitrogen i.e., atoms, molecules, ions, and electrons. The transport properties of this mixture were calculated as part of the program, as discussed in Ref. 40. It was suggested[41] that the high-heat transfer rates calculated by Scala were due to the small charge exchange cross section for the diffusion of nitrogen ions through nitrogen atoms utilized in this theory. This cross section, as used by Scala, was over 2 orders of magnitude smaller than the corresponding value calculated by Yos,[39] following the method of Mason.[42] Cross sections have been measured in rare gases[32] which are comparable to the latter two results.

Pallone has shown the foregoing premise to be correct.[6] He has used both the cross sections of Yos[39] and Scala[40] in calculations for nitrogen. A difference of more than a factor of 2 in the heat-transfer rates above 35,000 fps, and a difference of 2 orders of magnitude in the thermal conductivity resulted. Using the experimental thermal conductivity measurements in nitrogen obtained by Maecker[43] from arc experiments, Pallone shows close agreement with the heat-transfer rates calculated using the transport properties of Yos.[39]

It must be concluded from the data and discussion presented here that the predictions of Scala[5, 40] vary from other theories due to his choice of a charge exchange cross section which is considerably smaller than that calculated by Yos. Although the heat-transfer data presented in this paper are not capable of differentiating between the various theories, i.e., Pallone, Cohen, Hoshizaki, and Fay and Kemp, they certainly confirm the applicability of all of these theories as opposed to that of Scala. Consequently, the data are also an implicit verification of the transport properties of Hansen or Yos used in these calculations. At high temperatures the data of Yos appears preferable. It is also interesting to note that the simple binary diffusion model used by Fay and Kemp predicts that data trend as well as the more complex theories.

It is not as easy to identify the origin of the differences existing between the various experimental results shown in Fig. 16. There are now four sets of experimental data available which bear on this question. The present data are the most extensive and their validity can be judged from the earlier sections of this paper. The data of Offenhartz, et al.,[9] were obtained under conditions where the test time was questionable, or at best very short. The calculated test time for these experimental conditions was approximately 5 μsec and it has been our experience that approximately one-half this time is achieved. Hoshizaki[4] has presented data which verify his and the other similar theories. Although the data are not extensively documented in this reference, it is reasonable to assume from the conditions under which the experiments were performed that the data are valid.

Only the data of Warren[8] disagree with these three independent sets of data. Warren's data were obtained in an arc-driven shock tube in which the experimental test time was claimed to be precisely the value calculated for this shock tube in Ref. 10. It has been our experience that all measured shock tube test times are considerably shorter than those calculated from the theory of Roshko.[11] Even the data reported by Roshko, as well as the recent data of Hacker, et al.,[44] give experimental test times considerably shorter than the calculated value when corrected by using the boundary-layer calculations of Ref. 10. Warren's measurements were made with relatively thick calorimeter heat-transfer gages, which were made of a nickel alloy steel called Hytemco.# Although many of the differences between the techniques used by Warren and this paper were investigated, this difference could not be isolated. On the basis of the data presented, the high heat-transfer results of Warren must be considered to be anomalous, as the data from the three other independent investigations overwhelmingly support the lower heat-transfer levels.

Recently, Warren[50] has shown that the difference between the high heat-transfer rate data and the present paper is due to the gage material. Data from platinum calorimeters 0.002 in. thick agreed with the results of this paper, whereas Hytemco and nickel gages give the higher heating rates.

Summary

This experimental study has tried to deal with the difficulties which are encountered when shock tubes are operated in the high enthalpy range for the purpose of making heat-transfer measurements. We have presented our data in some detail to emphasize the difficulties and the limitations that are imposed on our ability to accumulate meaningful data. Although some questions have been left unanswered, the data which have been presented are shown to be valid, and techniques for making this determination are outlined.

The significance of the data is clear. The high heat-transfer rates predicted by Scala are not borne out by the data, and it must be concluded that the high thermal conductivity which he calculated was erroneous. The data do agree with, but cannot differentiate between, the theories of Fay and Kemp, Pallone, Cohen, and Hoshizaki, although they do favor the lower estimates at the high velocities. However, the differences between various calculations utilizing the same transport properties are of the same order as is the difference between the mean of the data and any one of the theories. It must also be concluded that there are no large unknowns in the transport properties of high temperature air up to 15,000°K and degrees of ionization of 50%, and these properties have been measured to a factor of 2 accuracy. The largest uncertainties remaining in the interpretation of these data involve the definition of the exact state of the gases as well as a better understanding of the transport properties of nitrogen and air and their differences.

References

[1] Adams, M. C., "A look at the heat transfer problem at supersatellite speeds," Avco-Everett Res. Lab. AMP 53 (December 1960); also ARS Rept. 1556-60 (1960).

[2] Bershader, D. and Rutowski, R. W., "Studies of an argon shock layer plasma," ARS Preprint 1998-61 (August 1961).

[3] Van der Noorda, R. S. L., "Heat transfer measurements from strongly ionized argon produced by strong shock waves," Cornell Univ. Graduate School of Aeronaut. Eng., Thesis (February 1957).

[4] Hoshizaki, H., "Heat transfer in planetary atmospheres at supersatellite speeds," ARS J. **32**, 1544–1552 (1962).

[5] Scala, S. M. and Warren, W. R., "Hypervelocity stagnation point heat transfer," ARS J. **32**, 101–102 (1962).

[6] Pallone, A. and Van Tassell, W., "The effects of ionization on stagnation-point heat transfer in air and in nitrogen," Avco Res. Advanced Dev. Div. RAD TM 62-75 (September 1962).

[7] Cohen, N., "Boundary layer similar solutions and correlation equations for laminar heat transfer distribution in equilibrium air at velocities up to 41,100 feet per second," NASA TR R-118 (1961).

[8] Warren, W. R., Rogers, D. A., and Harris, C. J., "The development of an electrically-heated shock driven test facility," MSVD Gen. Electric TIS Rept. R62SD37 (April 1962).

[9] Offenhartz, E., Weisblatt, H., and Flagg, R. F., "Stagnation point heat transfer measurements at super satellite speeds," J. Roy. Aeronaut. Soc. **66**, 53 (January 1962).

[10] Camm, J. C. and Rose, P. H., "Electric shock tube for high velocity simulation," Phys. Fluids **6**, 663–678 (May 1963).

[11] Roshko, A., "On flow duration in low pressure shock tubes," Phys. Fluids **3**, 835–842 (1960).

[12] Rose, P. H. and Stark, W. I., "Stagnation point heat transfer measurements in dissociated air," J. Aerospace Sci. **25**, 86–97 (1958).

[13] Vidal, R. J., "Model instrumentation techniques for heat transfer and force measurements in a hypersonic shock tunnel," Cornell Aeronaut. Lab. Rept. AD-917-A-1, Wright Air Dev. Center TN 56-315 (February 1956).

[14] Rose, P. H., "Development of the calorimeter heat transfer gage for use in shock tubes," Rev. Sci. Instr. **29**, 557–564 (July 1958).

[15] Camac, M. and Feinberg, R., "High speed infrared bolometer," Rev. Sci. Instr. **33**, 964–972 (September 1962).

[16] Hartunian, R. A. and Varwig, R. L., "A correction to thin-film heat transfer measurements," Aerospace Corp. Rept. TDR-594 (1217-01)-TN-2 (May 1961).

[17] Offenhartz, E. and Weisblatt, H., "Determination of the time history of the flow field about various blunt body shapes and sizes during experiments in 1.5-inch diameter shock tubes," Avco Res. Advanced Dev. Div. TR RAD TR-58-10 (July 1958).

[18] Teare, J. D., Georgiev, S., and Allen, R. A., "Radiation from the non-equilibrium shock front," *Progress in Astronautics and Rocketry: Hypersonic Flow Research* edited by F. R. Riddell (Academic Press Inc., New York, 1962) Vol. 7, pp. 281–317.

[19] Keck, J., Camm, J., Kivel, B., and Wentink, T., Jr., "Radiation from hot air, Part II," Ann. Phys. **7**, 1–38 (May 1959).

[20] Wray, K. L., "Chemical kinetics of high temperature air," *Progress in Astronautics and Rocketry: Hypersonic Flow Research* edited by F. R. Riddell (Academic Press Inc., New York, 1962) Vol. 7, pp. 181–204; also ARS Rept. 1975-61 (1961).

[21] Fay, J. A. and Riddell, F. R., "Theory of stagnation point heat transfer in dissociated air," J. Aerospace Sci. **25**, 73–86 (1958).

[22] Britton, D., Davidson, N , and Schott, G., "Shock waves in chemical kinetics," Faraday Soc. Discussion, no. 17, 58–68 (1954).

[23] Goodwin, G. and Chung, P. M., "Effects of nonequilibrium flows on aerodynamic heating during entry into the earth's atmosphere from parabolic orbits," Advan. Aeronaut. Sci. **4**, 997–1018 (September 1960).

[24] Wilson, J. A., "A shock tube measurement of the recombination rate of oxygen," Ph.D. Thesis, Cornell Univ. (June 1962).

[25] Wray, K. L., "Shock tube study of the recombination of O-atoms by Ar catalysts at high temperatures," J. Chem. Phys. **38**, 1518–1524 (April 1963).

[26] Inger, G. R., "Correlation of surface temperature effect on non-equilibrium heat transfer," ARS J. **32**, 1743–1744 (1962).

[27] Lin, S. C. and Fyfe, W. I., "Low-density shock tube for chemical kinetic studies," Phys. Fluids **4**, 238–249 (February 1961).

[28] Lin, S. C. and Teare, J. D., "Rate of ionization behind shock waves in air. II. Theoretical interpretation," Phys. Fluids **6**, 355–374 (March 1963).

[29] Bates, D. R., *Atomic and Molecular Processes* (Academic Press, Inc., New York, 1962), Chap. 7.

[30] Hartunian, R. A., "Theory of a probe for measuring local atom concentrations in hypersonic flows at low density," Aerospace Corp. Rept. TDR 930 (2230-06) TN-2 (April 1962).

[31] Fay, J. A. and Kemp, N. H., "Theory of stagnation point heat transfer in a partially ionized diatomic gas," IAS Preprint 63-60 (January 1963).

[32] Fay, J. A., "Hypersonic heat transfer in the air laminar boundary layer," Advisory Group for Aeronaut. Res. and Dev. Hypersonic Specialists' Conf., Brussels, Belgium (April 1962).

[33] Kivel, B. and Bailey, K., "Tables of radiation from high temperature air," Avco-Everett Res. Lab. Res. Rept. 21 (December 1957).

[34] Breene, R. G., Jr., Nardone, M., Reithof, T. R., and Zeldin, S., "Radiance of species in high temperature air," Gen. Electric MSVD TIS Rept. R62SD52 (July 1962).

[35] Myerott, R. E., Sokoloff, J., and Nicholls, R. W., "Absorption coefficients for air," Geophys. Res. Paper 58, GRD TN 60-277 (July 1960).

[36] Keck, J. C., Allen, R. A., and Taylor, R. L., "Electronic transition moments for air molecules," Symp. on Quantitative Spectroscopy at Elevated Temperatures and Selected Applications, Calif. Inst. Tech. (March 1963).

[37] Allen, R. A., Rose, P. H., and Camm, J. C., "Non-equilibrium and equilibrium radiation at supersatellite re-entry velocities," IAS Paper 63-77 (January 1963).

[38] Hansen, C. F., "Approximations for the thermodynamic and transport properties of high temperature air," NASA TR R-50 (1959).

[39] Yos, J. M., "Transport properties of nitrogen, hydrogen, oxygen and air to 30,000°K," Avco Res. Advanced Dev. Div., TM 63-7 (January 1963).

[40] Scala, S. M., "Heating problems of entry into planetary atmospheres from supercircular orbiting velocities," Gen. Electric TIS Rept. R61SD176 (October 1961).

[41] Private communication at NASA Headquarters, Washington, D. C. (June 1, 1962).

[42] Mason, E. A., Vanderslice, J. T., and Yos, J. M., "Transport properties of high-temperature multicomponent gas mixtures," Phys. Fluids **2**, 688–694 (1959).

[43] Maecker, H., "Experimental and theoretical studies of the properties of N_2 and air at high temperatures," AGARD Meeting, Braunschweig, Germany (1962).

[44] Hacker, D. S. and Wilson, L. N., "Shock tube results for hypersonic stagnation heating at very low Reynolds numbers," Armour Res. Foundation, Chicago, Ill., ARF A-44.

[45] Fenster, S. J. and Rozycki, R. C., "Heat transfer in a partially ionized laminar equilibrium air boundary layer," 8th Midwestern Mech. Conf., Cleveland, Ohio (April 1963).

[46] Fenster, S. J. and Heyman, R. J., "Heat transfer in a dissociated gas with variable heat of dissociation," Martin Co., Rept. R 62-16 (1962).

[47] Peng, T. and Pindroh, A. L., "An improved calculation of gas properties at high temperatures: air," Boeing Airplane Co., Doc. D2-11722 (1962).

[48] Gibson, W. E. and Marrone, P. V., "Correspondence between normal-shock and blunt-body flows," Phys. Fluids **5**, 1649–1656 (December 1962).

[49] Wittliff, C. E., Wilson, M. R., and Hertzberg, A., "The tailored-interface hypersonic shock tunnel," J. Aerospace Sci. **26**, 219–228 (1959).

[50] Gruszczynski, J. S. and Warren, W. R., "Experimental heat transfer studies of hypervelocity flight in planetary atmospheres," AIAA Preprint 63-450 (August 1963).

[51] Ziemer, R. W., "Instrumentation for magneto-aerodynamic heat transfer," Space Technology Labs., Physical Res. Lab., STL/TR-60-0000-09290 (September 1960).

[52] Phillips, W. R. and Valade, L. G., "Design of an infrared system for measuring stagnation point heat transfer rates in an electromagnetic shock tube," M.S. Thesis, U.S. Naval Postgraduate School, Monterey, Calif. (1959).